

Highlights from BNL and RHIC 2017

M. J. Tannenbaum *
Physics Department, 510c,
Brookhaven National Laboratory,
Upton, NY 11973-5000, USA
mjt@bnl.gov

1 Introduction

The Relativistic Heavy Ion Collider (RHIC) is one of the two remaining operating hadron colliders in the world, and the first and only polarized p+p collider. STAR is now the only experiment operating at RHIC. PHENIX ended its operation with the 2016 run and is now being dismantled. In its place a new experiment, sPHENIX, with a superconducting solenoid, a Hadron Calorimeter in the return yoke, an EMCal and small Hadron Calorimeter in the magnetic field as well as a Time Projection chamber for charged particle reconstruction and a silicon vertex detector (MAPS) (Fig. 1). sPHENIX goals are precision measurements of jets, heavy flavors and Upsilon spectroscopy.

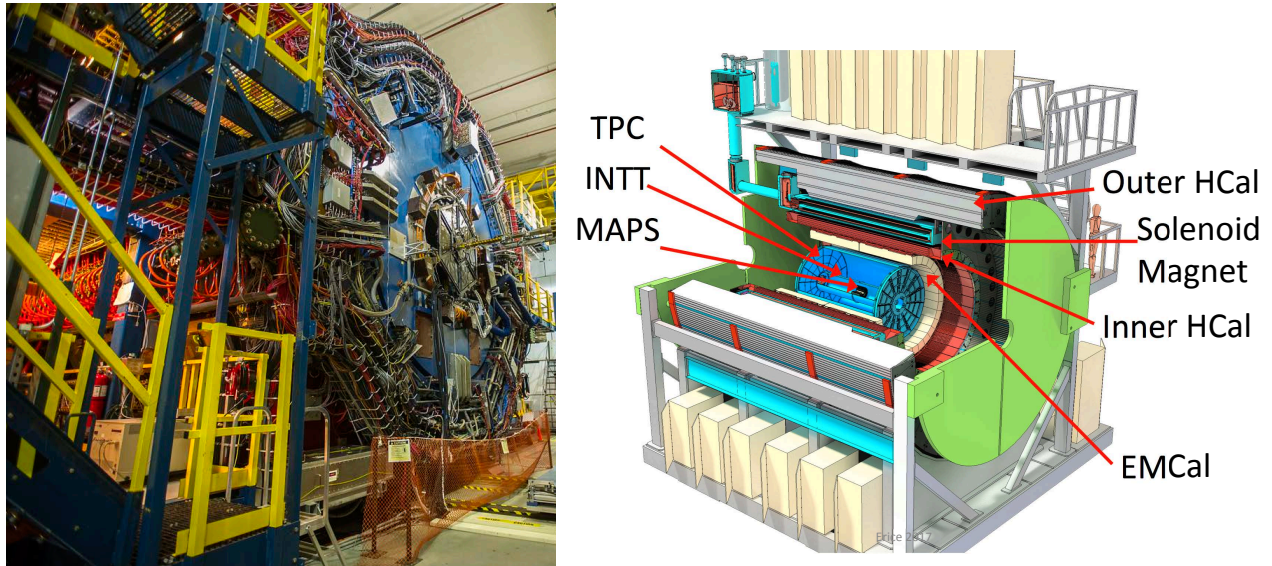


Figure 1: (left) STAR experiment and (right) proposed sPHENIX.

*Research supported by U. S. Department of Energy, DE-SC0012704.

2 Camp Upton 100 years; BNL 70, 1947-2017.

1948
A Pre-presidential Visit
Not-yet President of the United States Dwight D. Eisenhower visits the construction site of the Brookhaven Graphite Research Reactor.

1952 Strong Focusing
Brookhaven physicists analyze their Cosmotron and find it

1953
COSMOTRON
EXPERIMENTAL SET UP
Fig. 1. Experimental arrangement, showing disposition of the beams in both the long and short distance exposures.

1954
Conservation of Isotopic Spin and Isotopic Gauge Invariance*
C. N. Yang & R. L. Mills
Brookhaven National Laboratory, Upton, New York
(Received June 25, 1954)

1956
 K_L discovered

1957
Nobel Prize-winning Discovery: Parity Violation

1958
Helicity of Neutrons*
M. Goldhaber, L. Grodzins, and A. W. Sunyar
Brookhaven National Laboratory, Upton, New York
(Received December 11, 1957)

1960

1962
Nobel Prize-winning Discovery: The Muon-Neutrino

1964
Nobel Prize-winning Discovery: CP Violation

1964
 Ω^-

1965 HFBR Third Reactor for Research

Figure 2: Highlights in BNL History 1948–1965, starting with the visit of Dwight D. Eisenhower, then the president of Columbia University, in 1948. The other figures are labeled except perhaps for 1953—the Cosmotron, 1954—the Yang-Mills paper, 1958—Goldhaber, Grodzins, Sunyar, Helicity of Neutrons.

In 1917, the U.S. Army opened a training camp for soldiers before they were sent off to Europe to fight in World War I. This was Camp Upton near Yaphank on Long Island, 66 miles east of Manhattan. In World War II, Camp Upton was expanded and converted into a convalescent and rehabilitation hospital in September of 1944, and was put on surplus after the war ended. In 1947, the Associated Universities decided to put their proposed laboratory for constructing, and operating large scientific machines beyond the capabilities of single universities at Camp Upton, now BNL, starting with a nuclear reactor for research studies. In addition to the scientific achievements of BNL over the past 70 years, it is interesting to note that the famous U.S. composer Irving Berlin wrote many songs while he was at Camp Upton in 1917-18, which are still popular, most notably ‘God Bless America’, which is still played in the ‘7th inning stretch’ at Major League baseball games. Some achievements and discoveries at BNL are pictured in Fig. 2 for 1948-1965 and Fig. 3 for 1968-2005.

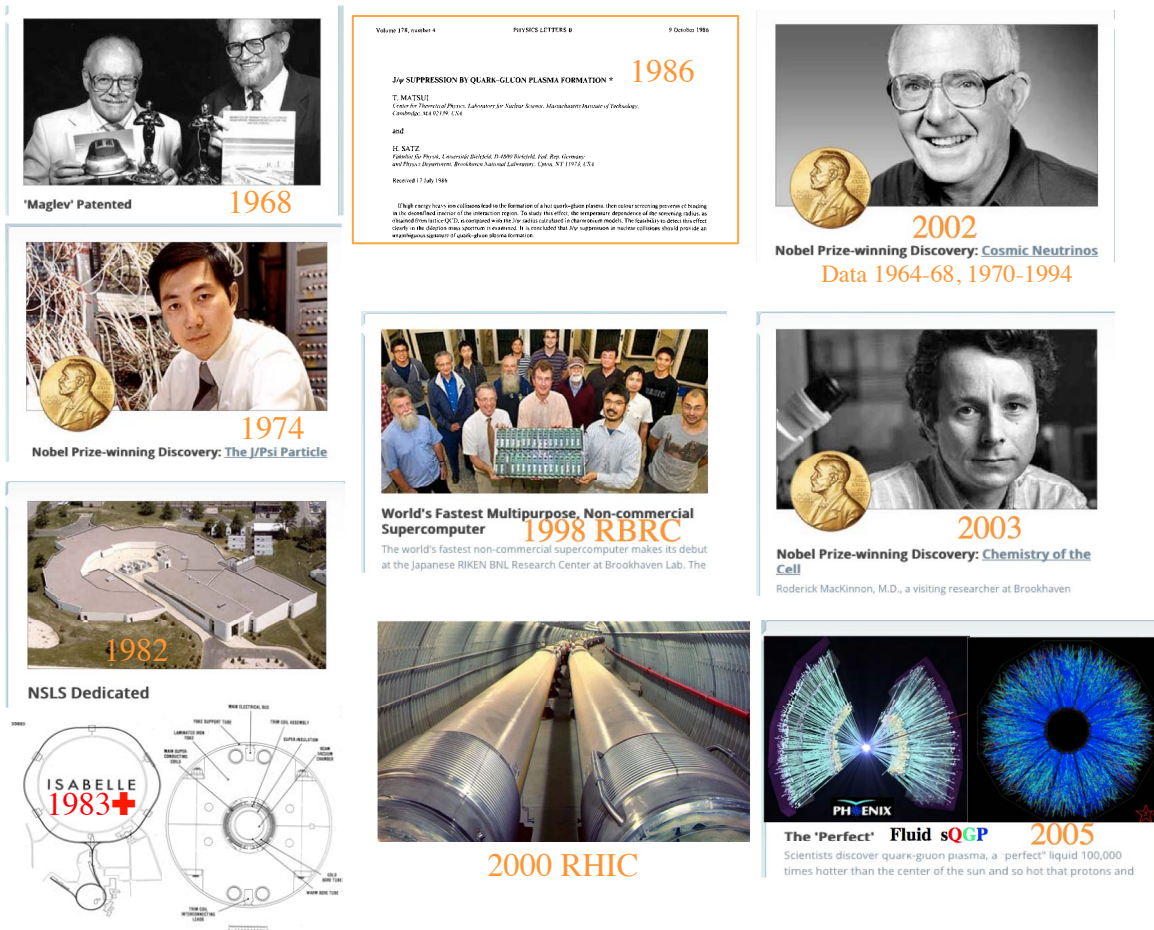
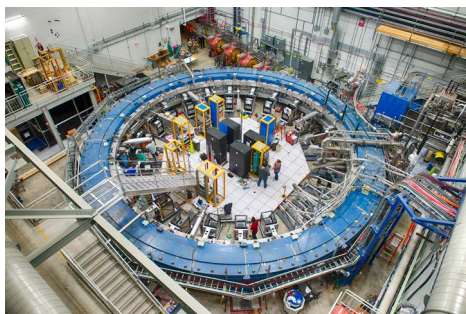


Figure 3: Highlights in BNL History 1968–2005 starting with the Patent of Maglev trains by Gordon Danby and James Powell. Next to the ISABELLE p+p collider, cancelled in 1983, is the profile of the Palmer Magnet [1], the basis of all subsequent superconducting collider magnets. 1986-Matsui Satz J/Ψ suppression, a signature of the Quark Gluon Plasma (QGP).

3 Muon g-2 experiment (from BNL) starts at Fermilab

Muon Magnet's Moment has Arrived
 The Muon g-2 experiment has begun its search for phantom particles with its world-famous and well-traveled electromagnet

June 1, 2017



The Muon g-2 ring with instrumentation, awaiting muons at Fermilab National Accelerator Laboratory. Credit: Fermilab

From the Fermilab press release: Getting to this point was a long road for Muon g-2, both figuratively and literally. The first generation of this experiment took place at the U.S. DOE's Brookhaven National Laboratory in New York State in the late 1990's and early 2000's.

Since it would have cost 10 times more to build a completely new machine at Brookhaven rather than move the magnet to Fermilab, the Muon g-2 team transported that large, fragile superconducting magnet in one piece from Long Island to the suburbs of Chicago in the summer of 2013.

As usual, press releases never get it right, perhaps the person who wrote the press release never heard of Charpak, Farley, Garwin, Muller, Sens and Zichichi [2].

3.1 Vorticity—Worthy of a Press Release

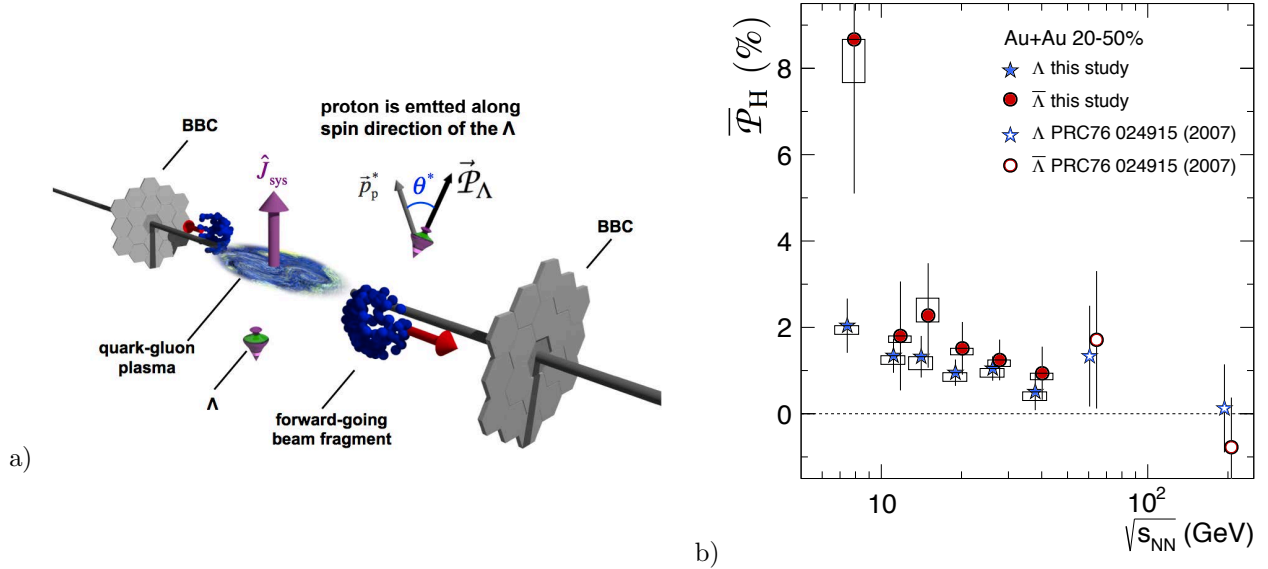


Figure 4: a) Schematic of forward and backward beam fragments passing each other and producing a magnetic field with direction \hat{j}_{sys} . b) Measured polarization \mathcal{P}_H with $H = \Lambda$ or $\bar{\Lambda}$ as a function of $\sqrt{s_{NN}}$.

One of the most interesting new results this year from RHIC [3] is a determination of the vorticity of the QGP in Au+Au collisions by measurement of the polarization \mathcal{P}_H of Λ hyperons with respect to the perpendicular of the reaction plane, which is the direction of the strong magnetic field (\hat{j}_{sys}) formed by the current loop of the highly charged nuclei passing each other (Fig. 4). The polarization is measurable because the Λ are generally produced polarized [4] and the proton in the decay $\Lambda \rightarrow p + \pi^-$ is emitted along the spin direction of the Λ . The average polarization of the Λ and $\bar{\Lambda}$ over $7 \leq \sqrt{s_{NN}} \leq 200$ GeV is $\bar{\mathcal{P}} \approx (1.2 \pm 0.2)\%$ from which the vorticity $\omega \approx 10^{22}/\text{s}$, which is 10^{15} times larger than any other fluid. On the other hand it is most interesting to note that the vorticity $\rightarrow 0$ at $\sqrt{s_{NN}} = 200$ GeV, where the QGP “the perfect liquid” was discovered, and increases to its largest values in the range $\sqrt{s_{NN}} = 7 - 19$ GeV of the CERN fixed target measurements—does this mean that they have an even more “perfect liquid”????

There are two other issues here that might be of interest to students: 1) calculate ω from the formula $\omega = kT\bar{\mathcal{P}}/\hbar$, where k is Boltzman’s constant, \hbar is Plank’s constant and T is the temperature of the QGP ≈ 300 MeV; 2) See CERN 86-07 for T.D. Lee’s story of how Jack Steinberger missed discovering parity violation in Λ decay from the reaction $\pi^- + p \rightarrow K^0 + \Lambda$.

4 RHIC operation in 2016 and future plans

BNL’s future plans for RHIC operation are given in Fig. 5. The main objectives until sPHENIX is working in ≈ 2022 is a run in 2018 with collisions of isobars, $^{96}_{40}\text{Zr} + ^{96}_{40}\text{Zr}$ compared to $^{96}_{44}\text{Ru} + ^{96}_{44}\text{Ru}$, to understand whether the charge separation of anisotropic flow v_2 of π^+ and π^- observed by STAR in Au+Au [5], the so-called Chiral Magnetic Effect, will be different for the different Z , hence due to the strong electromagnetic field in the nuclear collisions, or will remain unchanged for collisions of nuclei with the same number of

nucleons. In 2019 and 2020, STAR will then perform a beam energy scan searching for the QGP critical point and onset of deconfinement.

BNL's future plan 2017

Years	Beam Species and	Science Goals	New Systems
2014	Au+Au at 15 GeV Au+Au at 200 GeV ³ He+Au at 200 GeV	Heavy flavor flow, energy loss, thermalization, etc. Quarkonium studies QCD critical point search	Electron lenses 56 MHz SRF STAR HFT STAR MTD
2015-16	p↑+p↑ at 200 GeV p↑+Au, p↑+Al at 200 GeV High statistics Au+Au Au+Au at 62 GeV? d+Au @ 200, 62, 39, 20 GeV	Extract η/s(T) + constrain initial quantum fluctuations Complete heavy flavor studies Sphaleron tests Parton saturation tests	PHENIX MPC-EX STAR FMS preshower Roman Pots Coherent e-cooling test
2017	p↑+p↑ at 510 GeV	Transverse spin physics Sign change in Sivers function	Coherent e-cooling final
2018	No Run isobars	96Zr+96Zr and 96Ru+96Ru to test chiral magnetic effect on observed Au+Au charge separation effects	Low energy e-cooling install. STAR iTPC upgrade
2019-20	Au+Au at 5-20 GeV (BES-2)	Search for QCD critical point and onset of deconfinement	Low energy e-cooling
2022-23 2024-22	Au+Au at 200 GeV p↑+p↑, p↑+Au at 200 GeV	Jet, di-jet, γ-jet probes of parton transport and energy loss mechanism Color screening for different quarkonia Forward spin & initial state physics	sPHENIX Forward upgrades ?
2024-26 ≥ 2023 ?	Factor of 10 increase Au+Au No Runs Factor of 4 increase p+p	Complete above measurements	Transition to eRHIC

sPHENIX proposed run plan

Figure 5: BNL-RHIC run plan 2014–2026

RHIC Run	Year	Species	Energy	PHENIX Ldt
Run-1	2000	Au+Au	130 GeV	1 μb-1
Run-2	2001-2	Au+Au	200 GeV	24 μb-1
Run-2		Au+Au	19 GeV	0.4 μb-1
Run-3	2002/3	p+p	200 GeV	150 nb-1
Run-3		d+Au	200 GeV	2.74 nb-1
Run-3		p+p	200 GeV	0.35 nb-1
Run-4	2003/4	Au+Au	200 GeV	241 μb-1
Run-4		Au+Au	62.4 GeV	9 μb-1
Run-5	2005	Cu+Cu	200 GeV	3 nb-1
Run-5		Cu+Cu	62.4 GeV	0.19 nb-1
Run-5		Cu+Cu	22.4 GeV	2.7 μb-1
Run-6	2006	p+p	200 GeV	10.7 pb-1
Run-6		p+p	62.4 GeV	100 nb-1
Run-7	2007	Au+Au	200 GeV	813 μb-1
Run-8	2007/2008	d+Au	200 GeV	80 nb-1
Run-8		p+p	200 GeV	5.2 pb-1
Run-8		Au+Au	9.2 GeV	16 pb-1
Run-9	2009	p+p	200 GeV	16 pb-1
Run-9		p+p	500 GeV	14 pb-1
Run-10	2010	Au+Au	200 GeV	1.3 nb-1
Run-10		Au+Au	62.4 GeV	100 μb-1
Run-10		Au+Au	39 GeV	40 μb-1
Run-10		Au+Au	7.7 GeV	260 mb-1
Run-11	2011	p+p	500 GeV	27 pb-1
Run-11		Au+Au	200 GeV	915 μb-1
Run-11		Au+Au	27 GeV	5.2 μb-1
Run-11		Au+Au	19.6 GeV	13.7 M events
Run-12	2012	p+p	200 GeV	9.2 pb-1
Run-12		p+p	510 GeV	30 pb-1
Run-12		U+U	193 GeV	171 μb-1
Run-12		Cu+Au	200 GeV	4.96 nb-1
Run-13	2013	p+p (L)	510 GeV	156 pb-1
Run-14	2014	Au+Au	15 GeV	44.2 μb-1
Run-14		Au+Au	200 GeV	2.56 nb-1
Run-14		He3+Au	200 GeV	134 nb-1
Run-15	2015	p+p (L)	200 GeV	59.9 pb-1
Run-15		p+Au (T)	200 GeV	206.2 nb-1
Run-15		p+Al (T)	200 GeV	690.8 nb-1
Run-16	2016	Au+Au	200 GeV	14.3 G events
Run-16		d+Au	200 GeV	572Mcentevts
Run-16		d+Au	62.4 GeV	125Mcentevts
Run-16		d+Au	19.6 GeV	15Mcentevts
Run-16		d+Au	39 GeV	138Mcentevts
Run-17	2017	p+p (T)	510 GeV	~125 pb-1

RHIC energies, species combinations and luminosities (Run-1 to 16)

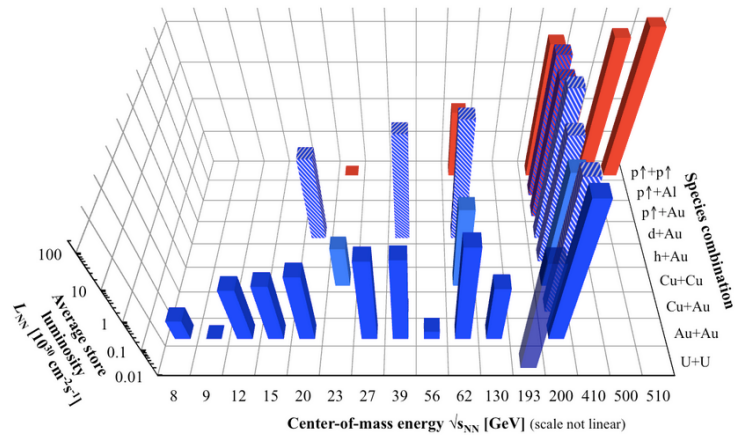


Figure 6: RHIC runs.

The history of RHIC runs is shown in Fig. 6. One may ask why the 2017 RHIC run is a

transversely polarized proton run when the original idea for spin physics at RHIC was based on single spin longitudinal (parity violating) asymmetries A_L of W^\pm production, since the W is coupled to flavor, not color like QCD.

4.1 The RHIC Spin Collaboration, Polarized Protons at RHIC

Ideas for a polarized proton collider (then ISABELLE) started at BNL during the famous Snowmass 1982 meeting [6] and continued, when ISABELLE became RHIC, with the formation of the RHIC Spin Collaboration [7], a group of experimental, theoretical and accelerator physicists with a common interest in spin, whose purpose was to add polarized proton capability to the Relativistic Heavy Ion Collider (RHIC). This idea came to fruition when, in 1995, RIKEN, the Institute of Physical and Chemical Research, in Japan decided to fund the spin hardware at RHIC and provide a second muon arm for the PHENIX experiment; and enhanced in 1997 when the RBRC (Fig. 7b) was founded at BNL, with T. D. Lee as director, with research focus on spin physics, Lattice QCD and Quark Gluon Plasma (QGP) physics by nurturing a new generation of young physicists.



Figure 7: a) BNL RSC originators (L–R) Gerry Bunce, Mike Tannenbaum, Thomas Roser, Yousef Makdisi, Satoshi Ozaki. b) T. D. Lee, founding director of the RIKEN BNL Research Center (RBRC).

The original goal of the RSC was that “Operation of RHIC with two beams of highly polarized protons (70%, either longitudinal or transverse) at high luminosity ($\mathcal{L} = 2 \cdot 10^{32} \text{ cm}^{-2} \text{ sec}^{-1}$ for two months/year will allow high statistics studies of polarization phenomena in the perturbative region of hard scattering where both QCD and ElectroWeak theory make detailed prediction of polarization effects.” It was expected that the integrated luminosity for two years (2×2 months) at would be $\int \mathcal{L} dt = 8 \times 10^{38} \text{ cm}^{-2}$ (800 pb $^{-1}$) at $\sqrt{s} = 500$ GeV [8]. The principal physics results to be obtained were Spin Structure Functions which require measurements to complement DIS electron measurements: a) Gluon ($G(x)$) and Gluon spin ($\Delta G(x)$) structure functions by inclusive γ and γ +Jet measurements; b) spin structure functions $\Delta \bar{q}$ from Drell-Yan, $\Delta \bar{u}$ from W^- and $\Delta \bar{d}$ from W^+ .

Following Bourrely and Soffer [9], the single longitudinal spin parity violating asymmetry of the W by flipping the spin of the proton is: $A_L^W = (1/P) \times (\sigma^- - \sigma^+)/(\sigma^- + \sigma^+)$, where

$\sigma = d\sigma^W/dy$ and the + or - signs refer to the spin along or opposite to the direction of the proton with polarization P (see Eq. 1) where $x_1 = \frac{m_W}{\sqrt{s}}e^y$, $x_2 = \frac{m_W}{\sqrt{s}}e^{-y}$.

$$A_L^{W^+}(y) = \frac{-\Delta u(x_1, M_W^2)\bar{d}(x_2, M_W^2) + \Delta\bar{d}(x_1, M_W^2)u(x_2, M_W^2)}{u(x_1, M_W^2)\bar{d}(x_2, M_W^2) + \bar{d}(x_1, M_W^2)u(x_2, M_W^2)} \quad (1)$$

and for $A_L^{W^-}(y)$ the $u \rightarrow d$ and $\bar{d} \rightarrow \bar{u}$.

The plan in PHENIX was to detect the reaction $u + \bar{d} \rightarrow W^+ \rightarrow e^+ + \nu_e$ at mid-rapidity and the decay $W^+ \rightarrow \mu^+ + \nu_\mu$ at forward rapidity $1.1 < |y| < 2.3$ and we thought that we could calculate the x of the W in these reactions. This led to some nice predictions for the results, circa 1995 (Fig. 8).

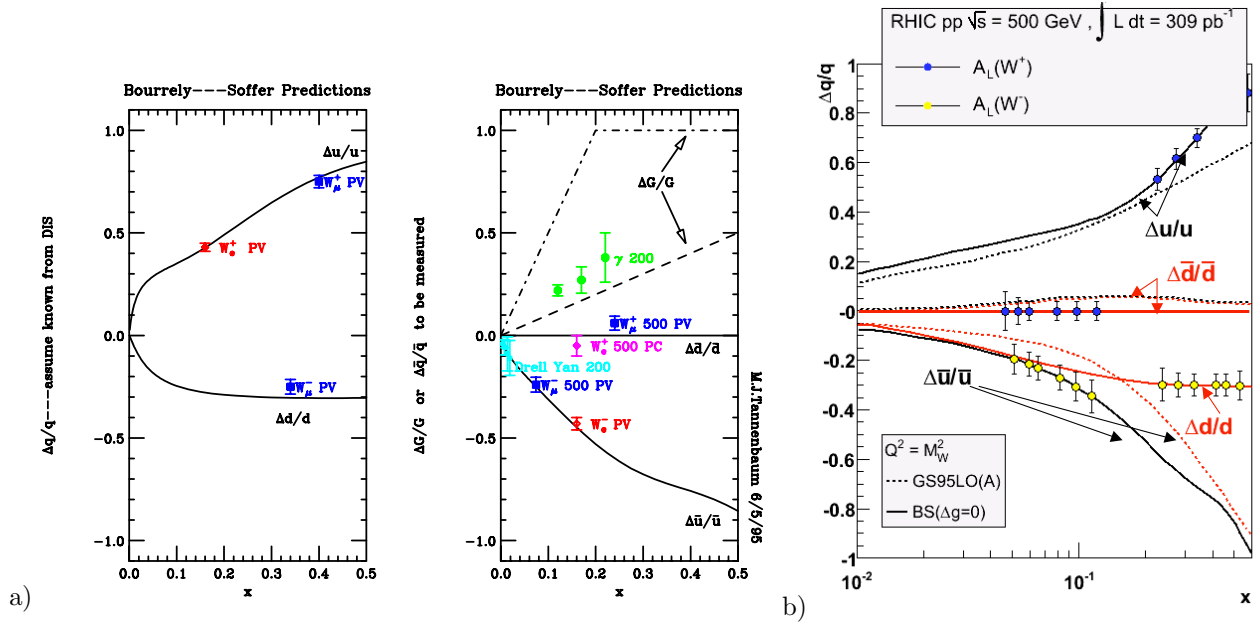


Figure 8: Expected results from W^\pm parity violating spin asymmetry, anti-quark and Gluon spin asymmetry c.1995: a) favoring mid-rapidity [8] with 800 pb^{-1} integrated luminosity at $\sqrt{s} = 500 \text{ GeV}$; b) favoring forward rapidity (only 309 pb^{-1}) [10]. Signs are reversed for W^\pm compared to Eq. 1.

We thought that we could calculate x_1 and x_2 in $p+p \rightarrow W^\pm + X$, followed by the leptonic decay. This works reasonably well for the μ at forward rapidity but there is a kinematic ambiguity for smaller rapidities (Fig. 9) as to whether the W is in the same or opposite direction to the e^\pm . However, this posed no problem for either PHENIX [11] or STAR [12] to measure W^\pm production for e^\pm at mid-rapidity with the Zichichi Jacobian peak [13].

Last year, STAR seems to have overcome the ambiguity with a measurement of the single transverse spin asymmetry A_N of the W^+ and W^- as a function of y_W over the range $|y_W| \leq 0.6$ (Fig. 9b) [14]. This measurement tests Transverse Momentum Dependent (TMD) parton distribution functions with respect to the ‘intrinsic’ transverse momentum k_T of partons in the proton. For example, the Sivers function is the correlation of k_T of a parton with the spin of the proton which may change sign according to the number of gluons exchanged in the reaction. Clearly this measurement from Run-11 is inadequate to draw a

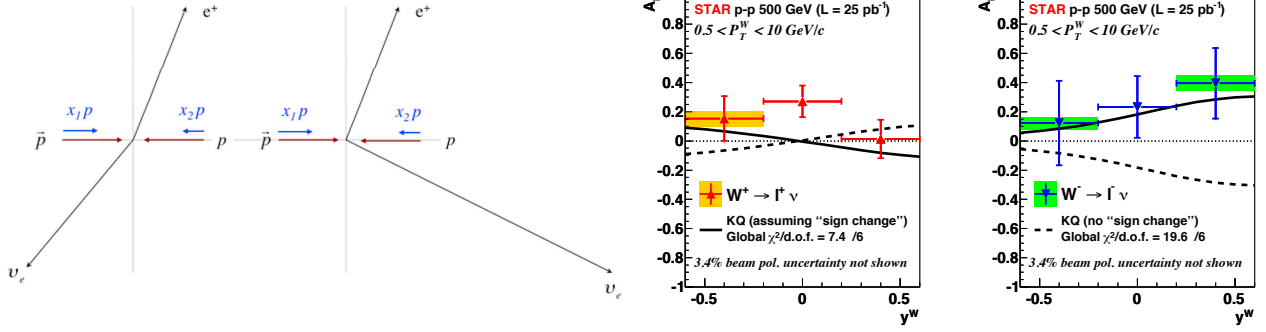


Figure 9: a) (left) Kinematic ambiguity of y^W for $W^+ \rightarrow e^+ + \nu_e$ with $y_e = +0.35$, $p_T^e = 35$ GeV/c: either $y_{\nu_e} = -0.73$ ($y^W = 0.19$) or $y_{\nu_e} = 1.43$ ($y^W = +0.89$). b) (right) Transverse single spin asymmetry as a function of rapidity y^W for W^+ and W^- from Run-11 $\int \mathcal{L} dt = 25$ pb $^{-1}$ [14].

firm conclusion; so the answer to the question following Fig. 6 (why transverse polarization to study TMD effects in Run-17 when the main thrust of the RSC is longitudinal polarization) is to get more data for Fig. 9b, with ≈ 100 pb $^{-1}$ collected.

For longitudinally polarized protons, the total collected luminosity at RHIC in Fig. 6 is ≈ 200 pb $^{-1}$, so decent results as in Fig. 8 should be forthcoming. However there may be a problem for future runs: the new U.S. President's proposed budget for 2018 terminates the RHIC spin program in order to fund the 'higher priority' 12 GeV JLAB science program. The budget also proposes to end U.S. participation in the LHC heavy ion program to focus funding on RHIC. The good news is that the U.S. congress has not yet acted on this budget at the present writing (November 2017) so these activities will continue until further notice (and hopefully beyond).

5 Heavy Ion Physics results at RHIC this past year.

Since the startup of RHIC in the year 2000, many discoveries have been made including the QGP as the perfect liquid. I present a quick summary and then move on to the latest results.

- Suppression of high p_T hadrons from hard-scattering of initial state partons; also modification of the away-side jet.
- Elliptic Flow at the Hydrodynamic limit with shear viscosity/entropy density at or near the quantum lower bound $\eta/s = 1/(4\pi) \implies$ QGP the Perfect Liquid.
- Elliptic flow of particles proportional to the number of the valence (constituent) quark count.
- Charged particle multiplicity proportional to the number of constituent quark participants.
- Higher order flow moments proportional to density fluctuations of the initial colliding nuclei.
- Suppression and flow of heavy quarks roughly the same as that of light quarks; QCD hard direct photons not suppressed, don't flow.
- Production and flow of soft photons $p_T < 2$ GeV/c with exponential distribution.

5.1 Flow in small systems

It was thought that elliptical flow, ($v_2 = \langle \cos 2\phi \rangle$), the emission of particles preferably along the short axis from the almond shape overlap region of the struck nucleons in an A+A collision (Fig. 10a) was an indication of a collective effect with hydrodynamic behavior related to the perfect liquid QGP . The results from Au+Au collisions at $\sqrt{s_{NN}} = 200$ GeV as a function of centrality (upper percentile) (Fig. 10b) [16] clearly indicate that v_2 decreases with increasing centrality of the collision as the overlap region becomes less elliptical.

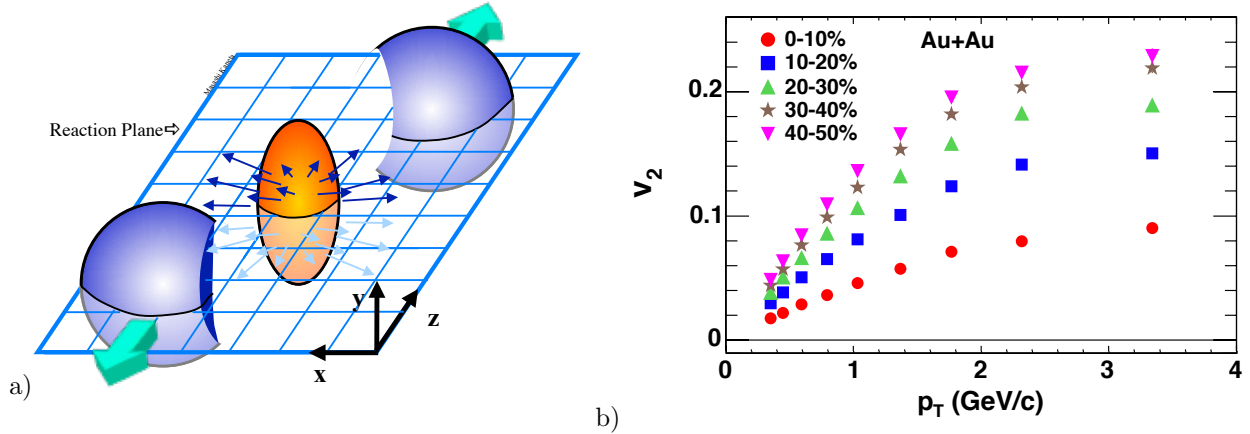


Figure 10: a) Almond shaped overlap zone generated just after an A+A collision where the incident nuclei are moving along the $\pm z$ axis. The reaction plane by definition contains the impact parameter vector (along the x axis, which defines $\phi = 0$) [15]. b) v_2 as a function of p_T for the centralities (0-10% is most central) indicated in Au+Au collisions at $\sqrt{s_{NN}} = 200$ GeV [16].

Measurements of small systems at RHIC namely d+Au and p+Au were initially used to establish baseline nuclear effects in which neither hot nuclear matter nor the QGP are produced [17]. However because v_2 depends on the geometry of the overlap region, it was decided to study whether small systems, p+Au, d+Au and ^3He +Au, produce collective expansion and flow related to their different collision geometries [18]. Recent results by PHENIX (Fig. 11) show that p+Au, d+Au and ^3He +Au with distinctly different initial geometries have similar if not identical values of v_2 as a function of p_T in collisions at $\sqrt{s_{NN}} = 200$ GeV and centrality 0-5%. Furthermore, ^3He +Au has a significant triangular flow, $v_3 = \langle \cos 3\phi \rangle$, which is significantly larger than the preliminary measurement of v_3 in d+Au.

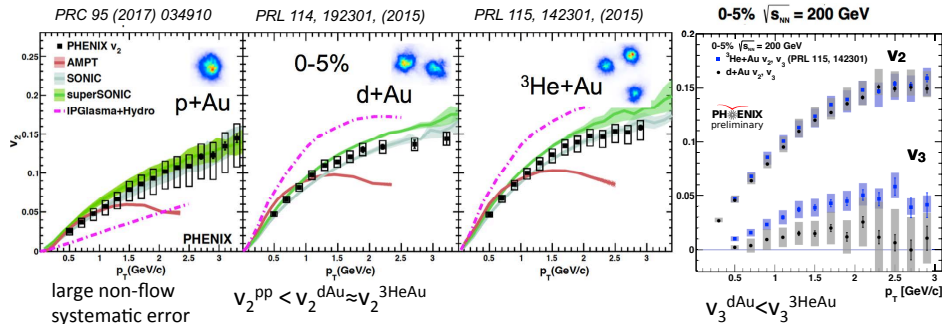


Figure 11: Anisotropic transverse flow in small systems indicated.

These results provide clear evidence that the v_2 measured in small systems arises from initial geometry coupled to interactions between medium constituents resulting in collective expansion. Especially noteworthy is that the v_2 vs. p_T values in the small systems at 0-5% centrality (Fig. 11) are actually greater than the v_2 vs. p_T values in Au+Au at comparable centrality (Fig. 10b), with obvious implication that there is still much to be learned about what is called ‘flow’ in collisions with nuclei.

5.2 A new detector and nice v_2 measurements of open charm (D^0) in Au+Au collisions by STAR, but ...

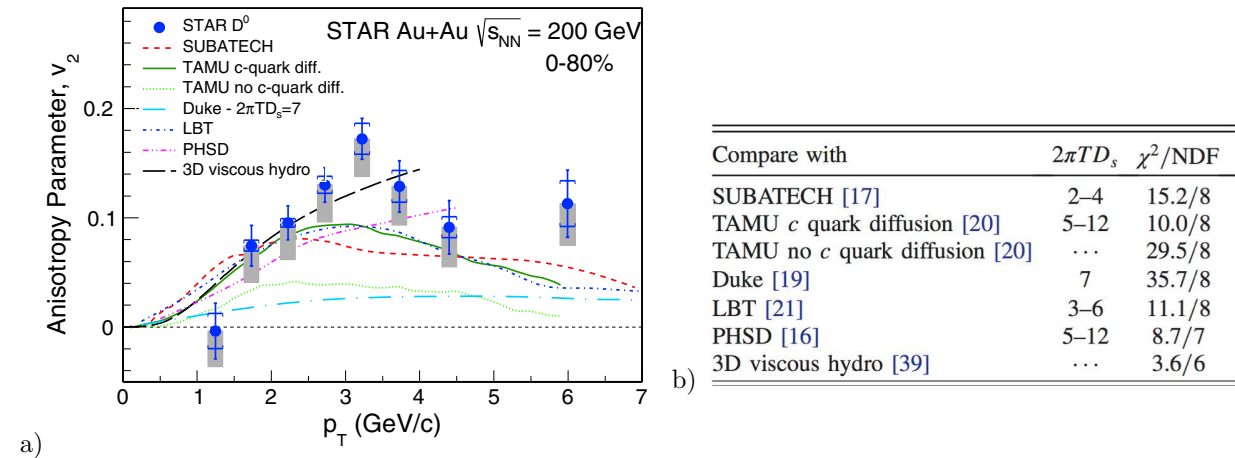


Figure 12: a) STAR v_2 of D^0 meson with theory calculations [19]. b) Table of Diffusion coefficients of theory calculations shown in (a) referring to numbered references in [19].

The first results from the STAR Heavy Flavor Tracker (HFT), a state of the art silicon vertex detector which includes the first use of Monolithic Active Pixel Sensors (MAPS), were published this year, a measurement of v_2 in open charm D^0 mesons [19] (Fig. 12a). Their conclusion was that: “Several theoretical calculations with temperature-dependent, dimensionless charm quark spatial diffusion coefficients ($2\pi TD_s$) in the range of $\sim 2 - 12$ (Fig. 12b) can simultaneously reproduce our D^0 v_2 result as well as the previously published STAR measurement of the D^0 nuclear modification factor [20]”.

5.2.1 ... but PHENIX did this 10 years ago with prompt single e^\pm from charm with numerical results: $\eta/s = (\frac{4}{3} \text{ to } 2)/4\pi \implies \text{QGP the Perfect Liquid.}$

In Fig. 13a, the PHENIX measurement [21] of the p_T spectrum of prompt single e^\pm from charm decay at mid-rapidity in p+p collisions at $\sqrt{s} = 200$ GeV is presented along with theory calculations in fixed-order-plus-next-to-leading-log (FONNL) pQCD [22], with the contributions from b and c quark decay indicated, in excellent agreement with the measurement. Fig. 13c [23] shows the suppression of single e^\pm in 0-10% centrality Au+Au collisions which is quantified by the nuclear modification factor $R_{AA} \equiv dN_{A+A}/(\langle T_{AA} \rangle d\sigma_{p+p})$, where dN_{A+A} is the differential yield in A+A collisions, $d\sigma_{p+p}$ is the differential cross section in p+p collisions at the same p_T , and $\langle T_{AA} \rangle$ is the average overlap integral of the nuclear thickness

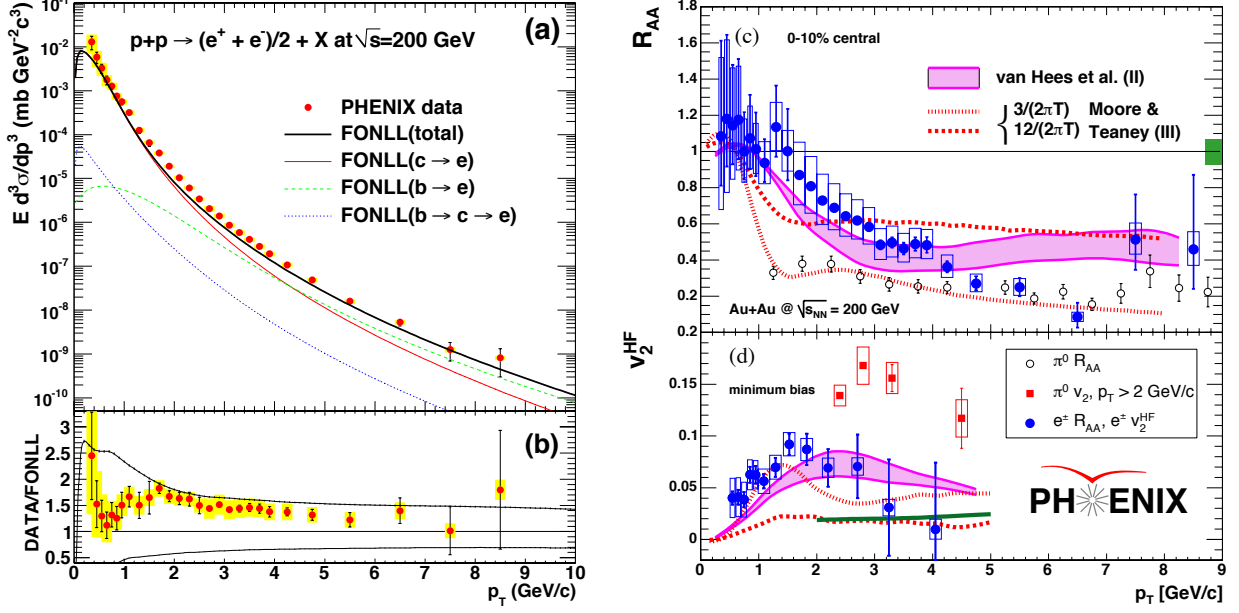


Figure 13: a) Invariant differential cross sections of electrons from heavy flavor quark decays [21]. The curves are FONLL calculations [22] b) The ratio of the measurement to the FONLL calculation. c) R_{AA} from direct-single e^\pm and π^0 [23] and d) elliptical flow v_2 for Heavy Flavor quarks and π^0 . Curves are theoretical predictions with the diffusion coefficient D [24],[25].

functions for the given centrality. Fig. 13d shows the measured v_2^{HF} for the single e^\pm from Heavy Flavor. Both R_{AA} and v_2^{HF} are compared to that of π^0 .

The observed flow of heavy quarks led Moore and Teaney [24] to suggest that the medium responds as a thermalized fluid and that the transport mean free path is small. They treated the heavy quark thermalizing as a diffusion problem with diffusion coefficient $D \approx 6\eta/(\varepsilon+p)$. The enthalpy $\varepsilon + p$ equals Ts at baryon chemical potential $\mu_B = 0$ so that $D = 6\eta/(Ts)$. When combined with the values $D = (6 \text{ to } 4)/(2\pi T)$ from curve II [25] on Fig. 13c,d the result is a value of $\eta/s \approx (2 \text{ to } 4/3)/(4\pi)$, intriguingly close to the conjectured quantum lower bound [26] $\eta/s \approx 1/(4\pi)$, hence the perfect liquid.

5.3 Jet Quenching: the first QCD based prediction BDMPSZ [27]

The first prediction of how to detect the QGP was via J/Ψ suppression [28] in 1986 (see Fig. 3). However the first QCD based prediction for detecting the QGP was BDMPSZ Jet Quenching [27]. This is produced by the energy loss, via LPM coherent radiation of gluons, of an outgoing parton with color charge fully exposed in a medium with a large density of similarly exposed color charges (i.e. the QGP) (Fig. 14a). Jet quenching was observed quite early at RHIC by suppression of high p_T π^0 [29], with lots of subsequent evidence (Fig. 14b). It is interesting to note that all identified hadrons generally have different R_{AA} for $p_T \leq 5$ GeV/c but tend to converge to the same value for $p_T \gtrsim 5$ GeV/c. The fact that direct- γ are not suppressed indicates that suppression is a medium effect on outgoing color-charged partons as predicted by BDMPSZ [27].

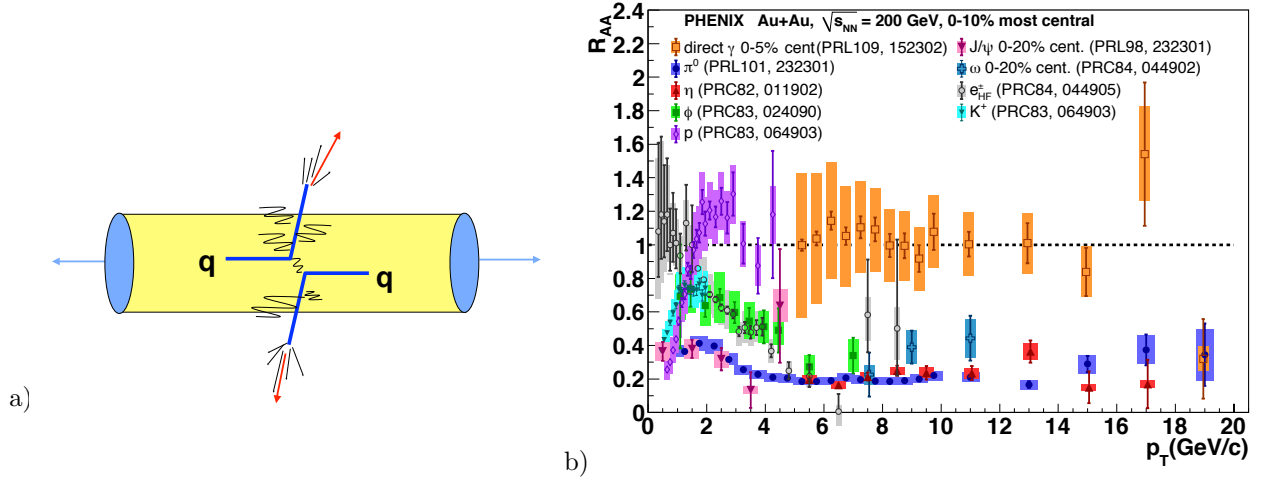


Figure 14: a) Schematic of $q+q$ scattering with scattered quarks losing energy in the medium. b) $R_{AA}(p_T)$ for all identified particles so far measured by PHENIX in Au+Au central collisions at $\sqrt{s_{NN}} = 200$ GeV.

5.3.1 But the BDMPSZ model has two predictions

(I) The energy loss of the outgoing parton, $-dE/dx$, per unit length (x) of a medium with total length L , is proportional to the total 4-momentum transfer-squared, $q^2(L)$, with the form:

$$\frac{-dE}{dx} \simeq \alpha_s \langle q^2(L) \rangle = \alpha_s \mu^2 L / \lambda_{\text{mfp}} = \alpha_s \hat{q} L \quad (2)$$

where μ , is the mean momentum transfer per collision, and the transport coefficient $\hat{q} = \mu^2 / \lambda_{\text{mfp}}$ is the 4-momentum-transfer-squared to the medium per mean free path, λ_{mfp} .

(II) Additionally, the accumulated momentum-squared, $\langle p_{\perp W}^2 \rangle$ transverse to a parton traversing a length L in the medium is well approximated by

$$\langle p_{\perp W}^2 \rangle \approx \langle q^2(L) \rangle = \hat{q} L \quad \text{so that} \quad \langle \hat{q} L \rangle / 2 = \langle k_T^2 \rangle_{AA} - \langle k_T'^2 \rangle_{pp} \quad (3)$$

since only the component of $\langle p_{\perp W}^2 \rangle \perp$ to the scattering plane affects k_T . This is called azimuthal broadening. Here (see Fig. 15) k_T denotes the intrinsic transverse momentum of a parton in a proton plus any medium effect and k_T' denotes the reduced value correcting for the lost energy of the scattered partons in the QGP, a new idea this year [30].

Even though jet quenching has been established and confirmed for more than 15 years, many experiments have tried to find azimuthal broadening at RHIC e.g. [31], [32], but have not been able to observe the effect because of systematic uncertainties.

5.3.2 Understanding k_T and k_T' .

In Fig. 15a, following the methods of Feynman, Field and Fox [33], CCOR [34] and PHENIX [35], the $\langle k_T^2 \rangle$ for di-hadrons is computed from Fig. 15a as:

$$\sqrt{\langle k_T^2 \rangle} = \frac{\hat{x}_h}{\langle z_t \rangle} \sqrt{\frac{\langle p_{\text{out}}^2 \rangle - (1 + x_h^2) \langle j_T^2 \rangle / 2}{x_h^2}} \quad (4)$$

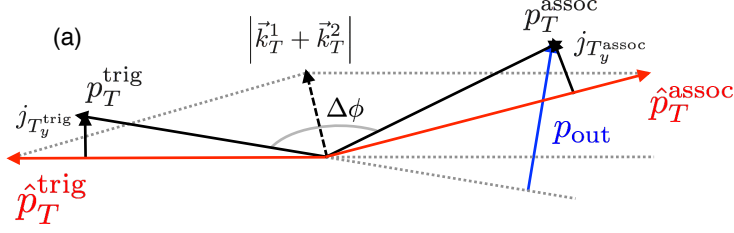


Figure 15: a) Initial configuration: trigger jet \hat{p}_{Tt} associated (away) jet \hat{p}_{Ta} with k_T effect (dashed arrow) and fragments p_{Tt} and p_{Ta} , with fragmentation transverse momentum j_{Ty} , and $p_{\text{out}} = p_{Ta} \sin(\pi - \Delta\phi)$.

where p_{Tt} , p_{Ta} are the transverse momenta of the trigger and away particles, $x_h = p_{Ta}/p_{Tt}$, $\Delta\phi$ is the angle between p_{Tt} and p_{Ta} and $p_{\text{out}} \equiv p_{Ta} \sin(\pi - \Delta\phi)$. The di-hadrons are assumed to be fragments of jets with transverse momenta \hat{p}_{Tt} and \hat{p}_{Ta} with ratio $\hat{x}_h = \hat{p}_{Ta}/\hat{p}_{Tt}$. $z_t \simeq p_{Tt}/\hat{p}_{Tt}$ is the fragmentation variable, the fraction of momentum of the trigger particle in the trigger jet. j_T is the jet fragmentation transverse momentum and we have taken $\langle j_{Tay}^2 \rangle \equiv \langle j_{Ta\phi}^2 \rangle = \langle j_{Tt\phi}^2 \rangle = \langle j_T^2 \rangle / 2$. The variable x_h (which STAR calls z_T) is used as an approximation of the variable $x_E = x_h \cos(\pi - \Delta\phi)$ from the original terminology at the CERN ISR where k_T was discovered and measured 40 years ago.

A recent STAR paper [36] on π^0 -hadron correlations in $\sqrt{s_{NN}} = 200$ GeV Au+Au 0-12% central collisions had very nice correlation functions for large enough $12 \leq p_{Tt} \leq 20$

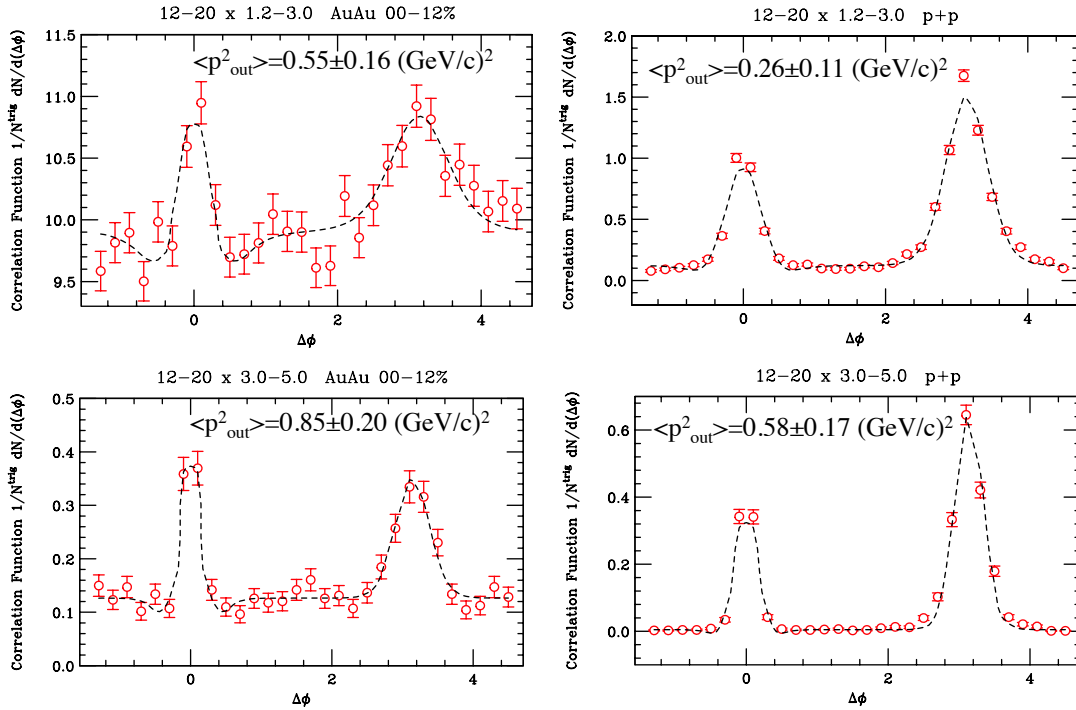


Figure 16: Fits to STAR π^0 -hadron correlation functions [36]: Gaussian in $\Delta\phi$ on trigger side ($\Delta\phi \approx 0$), and Gaussian in p_{out} on away side with fitted values of $\langle p_{\text{out}}^2 \rangle$ indicated.

GeV/c so that the v_2, v_3 modulation of the background was negligible (Fig. 16). I made fits to these data to determine $\langle p_{\text{out}}^2 \rangle$ so that I could calculate k_T in p+p and Au+Au using Eq. 4. The results for $3 \leq p_{T_a} \leq 5.0$ GeV/c were $\sqrt{\langle k_T^2 \rangle} = 2.5 \pm 0.3$ GeV/c for p+p and $\sqrt{\langle k_T^2 \rangle} = 1.4 \pm 0.2$ GeV/c, for Au+Au, exactly the opposite of azimuthal broadening (Eq. 3).

After considerable thought, I finally figured out what the problem was and introduced the new k'_T . For a di-jet produced in a hard scattering, the initial \hat{p}_{T_t} and \hat{p}_{T_a} (Fig. 15) will both be reduced by energy loss in the medium to become \hat{p}'_{T_t} and \hat{p}'_{T_a} which will be measured by the di-hadron correlations with p_{T_t} and p_{T_a} in Au+Au collisions. The azimuthal angle between the di-jets, determined by the $\langle k_T^2 \rangle$ in the original collision, should not change as both jets lose energy unless the medium induces multiple scattering from \hat{q} . Thus, without \hat{q} and assuming the same fragmentation transverse momentum $\langle j_T^2 \rangle$ in the original jets and those that have lost energy, the p_{out} between the away hadron with p_{T_a} and the trigger hadron with p_{T_t} will not change; but the $\langle k_T'^2 \rangle$ will be reduced because the ratio of the away to the trigger jets $\hat{x}'_h = \hat{p}'_{T_a}/\hat{p}'_{T_t}$ will be reduced. Thus the calculation of k'_T from the di-hadron p+p measurement to compare with Au+Au measurements with the same di-hadron p_{T_t} and p_{T_a} must use the values of \hat{x}_h , and $\langle z_T \rangle$ from the Au+Au measurement to compensate for the energy lost by the original dijet in p+p collisions.

The same values of \hat{x}_h , and $\langle z_t \rangle$ in Au+Au and p+p simplify Eqs. 3 and 4 to:

$$\langle \hat{q}L \rangle / 2 = \left[\frac{\hat{x}_h}{\langle z_t \rangle} \right]_{AA}^2 \left[\frac{\langle p_{\text{out}}^2 \rangle_{AA} - \langle p_{\text{out}}^2 \rangle_{pp}}{x_h^2} \right] \quad (5)$$

from which one could immediately get a reasonable answer for $\langle \hat{q}L \rangle / 2$ from the $\langle p_{\text{out}}^2 \rangle$ results indicated on Fig. 16 if the values of \hat{x}_h and $\langle z_t \rangle$ in the Au+Au measurement are known.

5.3.3 How to calculate $\langle \hat{q}L \rangle$ from the Au+Au (and p+p) measurements

At RHIC the π^0 high p_T spectra all have the same p_T^{-n} dependence, $n = 8.10 \pm 0.05$ in p+p and Au+Au collisions for all centralities measured at $\sqrt{s} = 200$ GeV [37]. From the Bjorken parent-child relation [38], the power n in p_T^{-n} is the same in the jet and fragment (π^0) p_T spectra. Also a triggered π^0 with p_{T_t} is weighted to higher $z_t = p_{T_t}/\hat{p}_{T_t}$, than $\langle z_t \rangle$ of a fragmentation function because the effective fragmentation function given p_{T_t} is biased by the steeply falling p_T spectrum to z_t^{n-2} times the unbiased fragmentation function. In any case $\langle z_T \rangle$ can be calculated from the measured π^0 p_T spectrum [35]. (For the present discussion, STAR measured $\langle z_t \rangle = 0.80 \pm 0.05$ from their p+p data [36].)

The ratio of the away jet to the trigger jet transverse momenta $\hat{x}_h = \hat{p}_{T_t}/\hat{p}_{T_a}$ can be calculated from the away particle $x_h = p_{T_a}/p_{T_t}$ distributions, which were also given in the STAR paper. The formula is [35]:

$$\left. \frac{dP}{dp_{T_a}} \right|_{p_{T_t}} = N(n-1) \frac{1}{\hat{x}_h} \frac{1}{(1 + \frac{x_h}{\hat{x}_h})^n} \quad (6)$$

This enabled me to calculate $\langle \hat{q}L \rangle$ from the $\langle p_{\text{out}}^2 \rangle$ results indicated on Fig. 16, now with sensible results (Table 1). The results in the two p_{T_a} bins are at the edge of agreement, different by 2.4σ , but both are $> 2.6\sigma$ from zero. These results leave several open questions, see Ref. [30] for the discussion. However there is a nice prediction of $\Delta\phi$ for for 35 GeV Jets

Table 1: Tabulations for \hat{q} -STAR π^0 -h PLB760(2016)689–696-MJT PLB(2017)

$\sqrt{s_{NN}} = 200\text{GeV}$	$\langle p_{Tt} \rangle$	$\langle p_{Ta} \rangle$	$\sqrt{\langle k_T^2 \rangle_{AA}}$	$\sqrt{\langle k_T^{\prime 2} \rangle_{pp}}$	$\langle \hat{q}L \rangle$
Reaction	GeV/c	GeV/c	GeV/c	GeV/c	GeV ²
Au+Au 0-12%	14.71	1.72	2.28 ± 0.35	1.01 ± 0.18	8.41 ± 2.66
Au+Au 0-12%	14.71	3.75	1.42 ± 0.22	1.08 ± 0.18	1.71 ± 0.67

at RHIC [39] for several values of $\langle \hat{q}L \rangle$ (Fig. 17). An amusing test would be to see if the present method gives the same answers for $\langle \hat{q}L \rangle$ by calculating $\langle p_{\text{out}}^2 \rangle$ of the predictions.

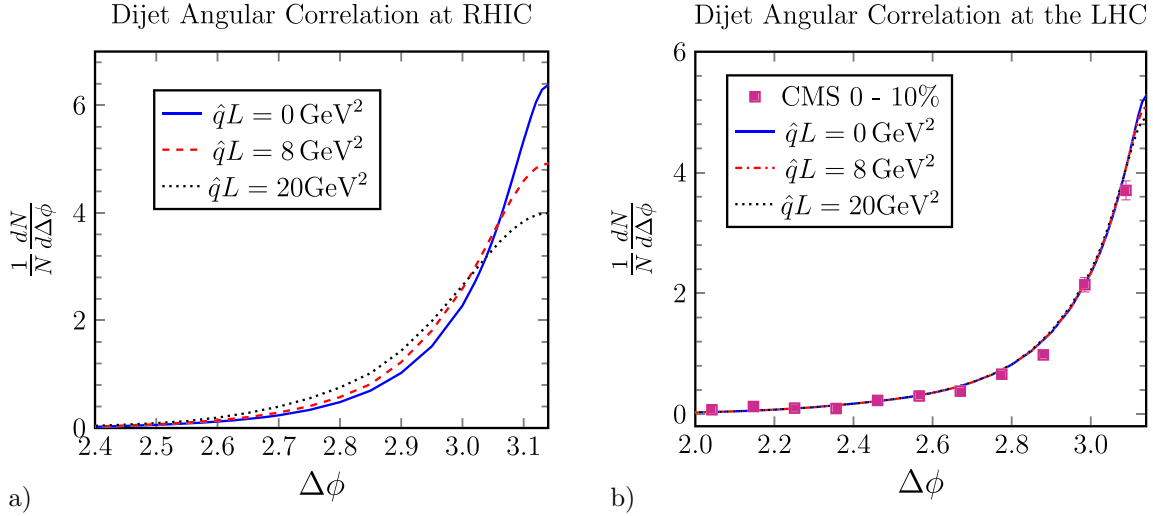


Figure 17: Prediction by Al Mueller and collaborators [39] of the di-jet azimuthal decorrelation as a function of $\hat{q}L$ for a) 35 GeV jets at RHIC $\sqrt{s_{NN}} = 200$ GeV; and b) 50 GeV jets at the LHC $\sqrt{s_{NN}} = 2.76$ TeV where “ p_T broadening effects are negligible” [39].

References

- [1] R. B. Palmer, E. J. Bleser *et al.*, Nucl. Instrum. Methods **A235** (1985) 435–463.
- [2] G. Charpak, F. J. M. Farley, R. L. Garwin, T. Muller, J. C. Sens and A. Zichichi, Nuovo Cimento **37** (1965) 1241-1363.
- [3] STAR Collab. (L. Adamczyk *et al.*), Nature **548** (2017) 62–66.
- [4] G. Bunce *et al.*, Phys. Rev. Lett. **36** (1976) 1113–1116.
- [5] STAR Collab. (L. Adamczyk *et al.*), Phys. Rev. Lett. **114** (2015) 252302.
- [6] M. J. Tannenbaum, *Waiting for the W and the Higgs*, Eur. Phys. J. **H41** (2016) 303–325.
- [7] Proceedings Polarized Collider Workshop, University Park, PA, 1990, Eds. J. Collins, S. F. Heppelman and R. W. Robinett, AIP Conf. Proc. 223 (AIP, New York, 1991).
- [8] M. J. Tannenbaum, Proc. Adiratico Research Conference on Trends in Collider Spin Physics, ICTP, Trieste, Italy, 5–8 December, 1995, Eds. Y. Onel, N. Paver and A. Penzo (World Scientific, Singapore, 1997) pp 31–53.

- [9] C. Bourrely and J. Soffer, Phys. Lett. B**314** (1993) 132–138.
- [10] Naohito Saito, pp 160–168 in Ref. [8].
- [11] PHENIX Collab. (A. Adare *et al.*), Phys. Rev. Lett. **106** (2011) 062001.
- [12] STAR Collab. (M. M. Aggarwal *et al.*), Phys. Rev. Lett. **106** (2011) 062002.
- [13] A. Zichichi, Proc. 12th International Conference on High Energy Physics, Dubna, Russia, 5–15 August, 1964 (Atomizdat, Moscow, 1966) Vol.2, p. 35.
- [14] STAR Collab. (L. Adamczyk *et al.*), Phys. Rev. Lett. **116** (2016) 132301.
- [15] PHENIX Collab. (M. Kaneta *et al.*), J. Phys. G**30** (2004) S1217–S1220.
- [16] PHENIX Collab. (A. Adare *et al.*), Phys. Rev. Lett. **98** (2007) 162301.
- [17] PHENIX Collab. (S. S. Adler *et al.*), Phys. Rev. Lett. **91** (2003) 072303. Also, see cover of PRL**91**, Issue 7, 15 August 2003, for d+Au measurements by all 4 RHIC experiments.
- [18] J. L. Nagle *et al.*, Phys. Rev. Lett. **113** (2011) 062002.
- [19] STAR Collab. (L. Adamczyk *et al.*), Phys. Rev. Lett. **116** (2016) 132301.
- [20] STAR Collab. (L. Adamczyk *et al.*), Phys. Rev. Lett. **113** (2014) 142301.
- [21] PHENIX Collab. (A. Adare *et al.*), Phys. Rev. Lett. **97** (2006) 252002.
- [22] R. Vogt, M. Cacciari and P. Nason, Nucl. Phys. A**774** (2006) 661–664.
- [23] PHENIX Collab. (A. Adare *et al.*), Phys. Rev. Lett. **98** (2007) 172301.
- [24] G. D. Moore and D. Teaney, Phys. Rev. C**71** (2005) 064904.
- [25] H. van Hees, V. Greco and R. Rapp, Phys. Rev. C**73** (2006) 034913.
- [26] P. K. Kovtun, D. T. Son and A. O. Starinets, Phys. Rev. Lett. **94** (2005) 111601.
- [27] R. Baier, D. Schiff and B. G. Zakharov, Ann. Rev. Nucl. Part. Sci. **50** (2000) 37–69.
- [28] T. Matsui and H. Satz, Phys. Lett. B**178** (1986) 416–422.
- [29] PHENIX Collab. (K. Adcox *et al.*), Phys. Rev. Lett. **88** (2001) 022301. Also, see cover of PRL**88**, Issue 2, 14 January 2002.
- [30] M. J. Tannenbaum, Phys. Lett. B**771** (2017) 553–557.
- [31] STAR Collab. (L. Adamczyk *et al.*), Phys. Rev. Lett. **112** (2014) 122301.
- [32] STAR Collab. (P. M. Jacobs, A. Schmah *et al.*), Nucl. Phys. A**956** (2016) 641–644.
- [33] R. P. Feynman, R. D. Field and G. C. Fox, Nucl. Phys. B**128** (1977) 1–65.
- [34] CCOR Collab. (A. L. S. Angelis *et al.*), Phys. Lett. B**97** (1980) 163–168.
- [35] PHENIX Collab. (S. S. Adler *et al.*), Phys. Rev. D**74** (2006) 072002.
- [36] STAR Collab. (L. Adamczyk *et al.*), Phys. Lett. B**760** (2016) 689–696.
- [37] PHENIX Collab. (A. Adare *et al.*), Phys. Rev. Lett. **101** (2008) 232301.
- [38] M. Jacob and P. V. Landshoff, Nucl. Phys. B**113** (1976) 395–412.
- [39] A. H. Mueller *et al.*, Phys. Lett. B**763** (2016) 208–212.